In order to improve on this schedule, the requisite generator information as stated in Sharma and Bahadoorsingh (2004) forms the necessary input data for the GMS implementation (see Table 1 for an example of input data for a simple four generator case). Applying the Hybrid SA solution method to this input data gives an improved maintenance schedule $\mathbf{x}^*$ that is described in Table 4. The fitness value for this schedule is $F^* = 265496$ which is a 5.9% improvement on the fitness value $F = 282148$ of the actual PowerGen maintenance schedule **x** utilised in 2013.

Table 4. An improved generator maintenance schedule for PowerGen in the year 2013

| **Generator #** | **Duration** (Week *i* to Week *j*) |
|---|---|
| 1 | 30 to 33 |
| 2 | 21 to 28 |
| 3 | 44 to 52 |
| 4 | 1 to 5 |
| 5 | 6 |
| 6 | 37 to 43 |
| 7 | 8 to 20 |
| 8 | 44 to 46 |
| 9 | 28 to 33 |
| 10 | 48 to 52 |
| 11 | 47 |
| 12 | 34 to 36 |
| 13 | 21 to 23 |
| 14 | 2 to 4 |
| 15 | none |
| 16 | 24 to 27 |
| 17 | 6 to 7 |
| 18 | 52 |

## 7. Conclusion

The numerical results given in Section 5 indicate that the local search methods rapidly converge to acceptable solutions of the GMS problem. The hybrid methods converge to marginally better solutions than those obtained by the local searches at the cost of significantly longer execution times. This suggests the following methodology in the application of our solution methods – local searches should be initially applied to obtain estimates of the fitness values of optimal solutions. The hybrid methods would then be used to obtain improved solutions.

In addition, the performance of the genetic algorithm is generally unacceptable when compared to our local search and hybrid methods. A similar comparison is made in Dahal and Chakpitak (2007). It is possible that further tuning of crossover and mutation parameters may improve the performance of a GA solution of the GMS problem. These modifications would be considered in future work.

## References:


Ahmad, A., and Kothari, D.P. (1998), "A review of recent advances in generator maintenance scheduling", *Electric Machines and Power Systems*, Vol.26, No.4, pp.373-387.

Dahal, K.P. and Chakpitak, N. (2007), "Generator maintenance scheduling in power systems using metaheuristic-based hybrid approaches", *Electric Power Systems Research*, Vol.77, No.7, pp.771-779.

Dawkins, R. (2006), *The Selfish Gene. 199*, Oxford University Press.

Egan, G.T, Dillon, T.S. and Morsztyn, K. (1976), "An experimental method of determination of optimal maintenance schedules in power systems using the branch-and-bound technique", *IEEE Transactions on Systems, Man, and Cybernetics*, No. 8. IEEE, pp.538-547.

Froger, A., Gendreau, M., Mendoza, J.E., Pinson, E. and Rousseau, L.M. (2015), "Maintenance scheduling in the electricity industry: A literature review", *European Journal of Operational Research*, Vol. 251, Issue 3, pp. 695-707.

Heylighen, F. and Chielens, K. (2009), "Evolution of culture, memetics", In: *Encyclopedia of Complexity and Systems Science*, Springer, p.3205-3220

Michalewicz, Z., and Fogel, D.B. (2013), *How to Solve It: Modern Heuristics*, Springer Science & Business Media.

Moscato, P., and Cotta, C. (2003), "A gentle introduction to memetic algorithms", In: *Handbook of Metaheuristics*, Springer, p.105-144.

Mukerji, R., Merrill, H.M., Erickson, B.W., Parker, J.H. and Friedman, R.E. (1991), "Power plant maintenance scheduling: Optimising economics and reliability", *IEEE Transactions on Power Systems*, Vol.6, No.2, pp.476-483.

Patton, A.D., and Ali, J. (1972), "Comparison of methods for generator maintenance scheduling", *IEEE PES Summer Meeting, Paper*, C 72 452-1, San Francisco, CA, July

Power Market Subcommittee (1979), "IEEE reliability test system", *IEEE Transactions on Power Apparatus and Systems*, No. 6, pp.2047-2054.

Rao, S.S. (2009), *Engineering Optimisation: Theory and Practice*. John Wiley & Sons.

Schlünz, E.B. (2011), *Decision Support for Generator Maintenance Scheduling in the Energy Sector*, PhD Thesis, Stellenbosch University.

Sharma, C. and Bahadoorsingh, S. (2004), "A MATLAB-based power generator maintenance scheduler", *Proceedings of the 2004 Power Systems Conference and Exposition*, IEEE PES, New York City, October, pp.1344-1348

Simon, D. (2013), *Evolutionary Optimisation Algorithms*, John Wiley & Sons.

Simon, D. (2015), *Evolutionary Optimisation Algorithms*, available at http://academic.csuohio.edu/simond/EvolutionaryOptimisation/.

Yellen, J., Al-Khamis, T.M., Vemuri, S., and Lemonidis, L. (1992), "A decomposition approach to unit maintenance scheduling", *IEEE Transactions on Power Systems*, Vol.7, No.2, pp.726-733.


## Authors' Biographical Notes:


Neil Ramsamooj *is a Lecturer at the Office of the Dean at the Faculty of Engineering at The University of the West Indies. In 2005, he completed the Ph.D. degree in Mathematics at the University of Wisconsin-Madison. His current research interests include optimisation techniques and applications of econometric methods.*

Laura Ramdath *is an Electrical Engineer at the Ministry of Works and Transport. She holds a BSc. in Electrical Engineering (Hons.) from The University of the West Indies, St. Augustine. Her*

*employment experience includes an engineering position of the Ministry of Public Administration and an internship at the Trinidad and Tobago Electricity Commissions.*

Sanjay Bahadoorsingh *is a Senior Lecturer at the Department of Electrical and Computer Engineering at The University of the West Indies. In 2009, he completed the Ph.D. degree at The University of Manchester. His areas of research are power systems, asset management and dielectric aging.*

Chandrabhan Sharma *is the Professor of Energy Systems with the Faculty of Engineering, The University of West Indies. He is the Head of the Centre for Energy Studies and the Leader of the Energy Systems Group. He has served as a member of the Board of Directors of the local Electric Utility for over 10 years and as a member of the Board of Directors of the largest bank in the country. Prior to joining the Academic staff at the university, he was attached to the petrochemical industry in Trinidad. His interests are in the area of power system operations and control.*

■

**ISSN 0511-5728**
*The West Indian Journal of Engineering*
Vol.41, No.2, January 2019, pp.13-21

# Determination of Best-fit Propagation Models for Pathloss Prediction of a 4G LTE Network in Suburban and Urban Areas of Lagos, Nigeria

Agbotiname L. Imoize [a,Ψ], Augustus E. Ibhaze[b], Peace O. Nwosu[c], and Simeon O. Ajose[d]

Department of Electrical and Electronics Engineering, Faculty of Engineering, University of Lagos, Akoka Lagos, Nigeria

[a]E-mail: aimoize@unilag.edu.ng;
[b]E-mail: ibhazea@gmail.com;
[c]E-mail: peacelink345@yahoo.com;
[d]E-mail: solumideajose@gmail.com

[Ψ] *Corresponding Author*

*(Received 30 December 2017; Revised 01 June 2018; Accepted 10 July 2018)*

**Abstract:** *Propagation measurements and modeling provide useful information for signal strength prediction and the design of transmitters and receivers for wireless communication systems. In order to deploy efficient wireless communication systems, path loss models are indispensable for effective mobile network planning and optimisation. This paper presents propagation models suitable for path loss prediction of a fourth generation long-term evolution (4G LTE) network in the suburban and urban areas of Lagos, Nigeria. The reference signal received power (RSRP) of a 4G LTE network was measured at an operating frequency of 3.4GHz, and measured data was compared against existing pathloss models. Among the candidate models, the COST 231-Hata and the Ericsson models showed the best performances in the urban and suburban areas with root mean squared errors (RMSEs) of 5.13dB and 7.08dB, respectively. These models were selected and developed using the least square regression algorithm. The developed models showed good prediction results with RMSEs of 6.20dB and 5.90dB in the urban and suburban areas, respectively, and compare favourably with propagation measurement results reported for similar areas. It was found that these models would better characterise radio coverage and mobile network planning, enhancing the quality of mobile services in related areas.*

***Keywords:*** *4G LTE network; Path loss modeling; Propagation models; Suburban; Urban area, Least square regression*

## 1. Introduction

Propagation modeling has attracted major concerns in the industry and academia in recent years. Path loss models are essential tools for signal strength estimation, a key performance indicator for radio system installation within a wireless communication environment (Athanasiadou, 2009). As electromagnetic waves radiate through space, the signal strength degrades due to the signal path distance, and dynamic terrain characteristics. This results in signal scattering, absorption and reflection among others. It is worthy of note that these models are site specific and are designed based on the propagation terrain of the environment of interest (Mollel and Kisangiri, 2014).

In addition, slight deviations in the characterisation of the area under investigation could affect the efficiency of propagation models designed for the area. This implies that the adoption of models in environments other than those designed for their application could result in severe planning and performance issues. Fourth generation long-term evolution (4G LTE) technology has an undeniable capacity for wireless broadband services due to its enormous benefits. The key features of 4G LTE include higher data rates, greater spectral efficiency, low latency, scalable bandwidth, reduced network complexity and improved quality of service, resulting in user satisfaction (Song and Shen, 2010; Shabbir, et al., 2011; Ramiro and Hamied, 2011; Dahlman, Parkvall, and Skold, 2013; ElNashar, El-Saidny and Sherif, 2014).

However, it is quite challenging to decide on the path loss model applicable to the environment of interest. There are very few proposed models for the 4G LTE contest with a focus on the 3.4 GHz frequency band, but we have not seen any elaborate study on propagation modeling of 4G LTE network with a focus on the Nigerian environment. Therefore, the focus of this paper is to investigate the relationship between measured pathloss and existing propagation models, with a goal to determining the best models for a commercial 4G LTE network in the suburban and urban areas of Lagos, Nigeria. This would be very useful to mobile network planners and engineers in ensuring greater accuracy and better quality of service deployment in the suburban and urban areas of Lagos, Nigeria. The results presented in this paper could be very useful in predicting and characterising propagation path loss in the Nigerian environment, and our future work will focus on providing correction factors to ease the applicability of the proposed models in different areas.

This paper is organised as follows. Section 2 presents an overview of related works on propagation

measurements and channel modeling. Section 3 covers the measurements campaigns, experimental set-up, and modeling parameters. Section 4 presents the results of the study and useful discussions. Finally, the conclusion to the paper is given in Section 5.

## 2. Related Work

Long Term Evolution, a 3rd generation partnership project (3GPP), has been designed and developed to meet the requirements of mobile network operation at data rates up to 100Mbps (Dimou et al., 2009). This will enable operators to provide high data rate applications with low latency, thereby culminating into an increased market penetration by mobile operators (Sesia, Baker and Toufik, 2011). Different propagation models have been adapted to different terrains at different frequencies, and the classification of models into urban, suburban and open (rural) areas has been reported in (Abhayawardhana et al., 2005; Ajose and Imoize, 2013). These models include the free space model, Okumura Hata model, COST 231 model, Walfish-Ikegami model, Lee model, Stanford University Interim (SUI) model, ECC-33 model and others (Milanovic, Rimac-Drlje and Beyuk, 2007; Aragon-Zavala, 2008; Molisch, 2012).

The performance efficiency of the existing models when applied to wireless terrains other than those they were designed for falls far from ideal (Chebil et al. 2011). Thus, this prompts the need to determine the models that best predict the signal strength of the wireless channel. Several studies conducted in Nigeria and other parts of the world have revealed that a number of path loss models perform efficiently when tuned with respect to measured data.

On propagation measurements and channel modeling, Ajose and Imoize (2013) reported extensive propagation measurements, and presented a modified COST 231 Hata model for improved pathloss prediction in Lagos, Nigeria. Similarly, Ibhaze et al. (2016) conducted measurement campaign at 1800 MHz in Ikorodu, Nigeria, and proposed the modification of SUI and COST 231 models for signal prediction and network planning in the investigated area.

Chebil, Lawas, and Islam (2013) carried out a set of measurements at frequencies ranging from 1800 MHz to 1900MHz and compared the measured pathloss with six empirical propagation models. It was reported that the SUI and the lognormal models showed superiority over other models, and could be used to estimate the predicted path loss in microcell mobile coverage, in the Malaysian environment.

Kamboj, Gupta and Birla (2011) reported that the SUI path loss model provides the minimum path loss among other path loss models compared under specified conditions, using propagation measurements at 3.5GHz. Similarly, Kale and Jadhav (2013) performed analysis of empirical models for WiMAX in an urban environment in India. It was reported in the study that the Ericsson and the SUI models showed a better performance in the investigated urban environment.

Bola and Saini (2013) carried out measurement campaigns using different empirical models for WiMAX in urban areas. The analysis showed that all models experienced higher path loss due to multipath and non-line of sight (NLOS) environments. It was concluded that there is a slight change in path loss when the operating frequency was changed. Further studies on LTE, WiMAX, WLAN design, and performance analysis are reported in (Korowajczuk, 2011; Katev, 2012).

In another related study, Podder et al. (2012) reported an analytical study on propagation models at 2.5GHz. The comparative analysis revealed that increased multipath in the urban and suburban areas favored the SUI model, which experienced the lowest path loss compared to the rural area. In the rural area, the COST-Hata model provided the lowest path loss compare to the SUI model, and the results showed that no single propagation model is well suited for all the tested areas.

On performance analysis of diverse models for wireless network in different environments, Khan, Eng, and Kamboh, (2012) reported that all models under study in urban areas, due to increased multipath effect and NLOS, experienced higher path loss compared to suburban areas, and that no single model could be recommended for all environments.

Famoriji and Olasoji (2013) used Friis and Okumura - Hata models to predict broadcasting signal strength for a television station in Akure Ondo State, Nigeria. The authors concluded that the performance of Okumura–Hata model showed its suitability for good signal prediction and the mean deviation errors were added to the Okumura-Hata model in order to derive the modified Okumura-Hata model suitable for deployment in the Akure metropolis.

Furthermore, Ibhaze et al. (2017) proposed the modification of Ericsson model at 2100MHz for the Alagbado axis of Lagos, Nigeria. Here, higher degree polynomial was fitted to measured data and the results were compared with some empirical models. Although this model was used earlier in predicting lower frequency ranges other than the investigated spectrum, it predicted the investigated wireless channel with less probability of error in contrast to the previously used Okumura-Hata model, and inappropriate model application was seen to have resulted in marked quality and coverage issues.

## 3. Measurement Campaigns

Measurement campaigns at 3.4 GHz using a personal computer with Genex probe, a data collection software interface and a GPS unit for the receiving device tracking is presented in the experimental set-up as shown in Figure 1, and a typical eNodeB site is as shown in Figure. 2.

**Figure 1.** Experimental set-up inside a drive test vehicle

**Figure 2.** Pictorial view of a typical eNodeB site located in Ajah area of Lagos, Nigeria

The reference signal received power measurements were taken and stored on a personal computer (PC) which had GENEX probe drive test (DT) software installed on it, and a Huawei Model E392 (4G compatible). The operating frequency is set from the PC and other readings such as transmitter-receiver distance, received signal level, location (latitude and longitude) are read from the PC. Here the personal computer with GENEX software installed on it, the Huawei modem and the GPS system were set-up in the drive test vehicle. The channel frequency was set to 3.4GHz, and the reference distance used for the measurements is 100m from the fixed base station. Transmitter to receiver distance was varied between 0.1km to 1.0km in steps of 50m at a near constant receiver antenna height of 1.5m. The transmitter-receiver distance was limited to 1km, in order to limit the impact of interference from neighboring transmitting antennas.

### 3.1 Suburban Areas

Propagation measurements were carried out at two eNodeB sites located in Ajah, typical of a suburban area in Lagos, Nigeria. Ajah is located on Latitude 6.4670N and Longitude 3.5670E. This area is dominantly residential and moderately congested. In addition, there are several schools, banks, and religion worship centers in this area. A typical Ajah area on a Google map is shown in Figure 3. The tested eNodeB sites are as shown in Figure. 4 and for simplicity, these are labelled as eNodeB 1 and eNodeB 2.

**Figure 3.** Google map showing Ajah (suburban) area of Lagos Nigeria

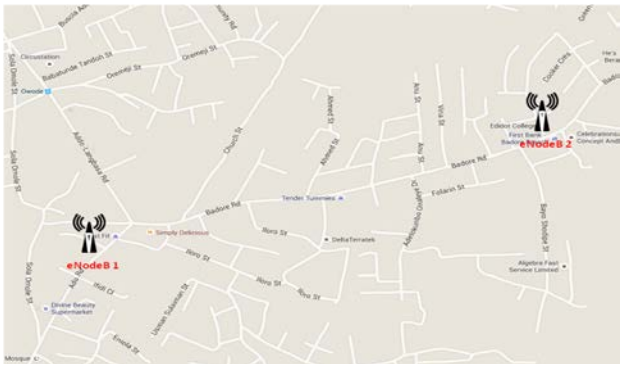


**Figure 4.** Google map showing the location of eNodeBs in the suburban areas

### 3.2 Urban Areas

Field measurements were carried out at two sites in Lagos-Island typical of an urban area in Lagos. Lagos-Island is located on Latitude 6.4500N and Longitude 3.4000E and is classified as an urban area. This area is dominantly a business hub with high density of high-rise buildings. A typical Lagos-highland area on a Google map is shown in Figure 5. The eNodeB sites location are as shown in Figure 6 and for convenience, these are denoted as eNodeB 3 and eNodeB 4.

**Figure 5.** Google map showing Lagos-highland (urban) areas of Lagos Nigeria

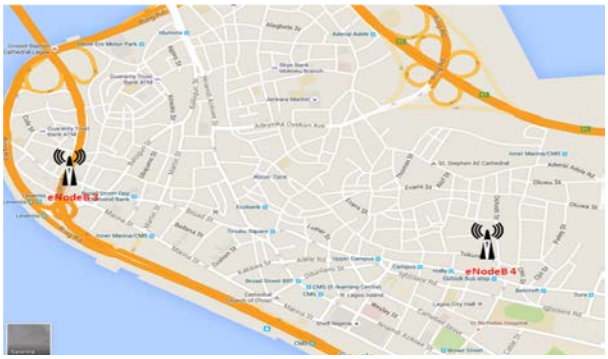


**Figure 6.** Google map showing the location of eNodeBs in the urban areas

## 4. Modelling Parameters

In this study, the operating frequency is fixed at 3400 MHz, distance between the transmit antenna and the receiver is limited to 1km with a transmitter height of 20m in urban area and 24m in sub-urban areas. Evidence shows that 1km is a reasonable antenna separation distance to limit the impact of interference from adjacent base stations (eNodeBs). For the Lagos environment, average inter-building distance is about 20m and street width is about 10m. Correction factors for shadowing effects are given as 10.6 dB in urban and 8.2dB in sub-urban areas, respectively (Sesia, Baker and Toufik, 2011; Shabbir et al., 2011). The modeling parameters are as shown in Table 1.

**Table 1.** Modeling Parameters

| Parameters | Values | |
|---|---|---|
| | Suburban area | Urban area |
| Transmitter power | 43 dBm | 43 dBm |
| Operating frequency | 3.4GHz | 3.4GHz |
| Max. distance between Tx and Rx | 1km | 1km |
| Transmitter antenna height | 20m | 24m |
| Receiver antenna height | 1.5m | 1.5m |
| Building to building distance | 20m | 20m |
| Average building height | 9m | 18m |
| Street width | 10m | 10m |
| Street orientation angle | $40^o$ | $30^o$ |
| Correction for shadowing | 8.2dBm | 10.6dBm |

## 5. Results and Discussion

The mean reference signal received power measured from the suburban and urban areas was converted to the equivalent pathloss values for further analysis. Results shown as tests eNodeB 1 and eNodeB 2 are used for analysis to reflect a suburban area, and tests eNodeB 3 and eNodeB 4 are typical of an urban area. The path loss is calculated using Eq. (1) as in Rappaport (1996).

$$PL(dB) = P_T + G_T + G_R - P_R - L_T - L_R \quad (1)$$

where,

$$P_T + G_T + G_R - L_T - L_R = EIRP \quad (2)$$

From Equations (1) and (2),

$$PL(dB) = EIRP - P_R \quad (3)$$

Equation (1) gives the gains and losses in the signal strength from the transmitter to the receiver, and Table 2 presents the LTE downlink gains and losses (Mishra, 2004). The total effective isotropically radiated power (EIRP) includes the transmitter EIRP, and other gains and losses. The values of the test eNodeB parameters are observed from the equipment manufacturers' manual, actual measurements and from the data reported in (Mishra, 2004; Holma and Toskala, 2007). From Table 2, the total EIRP is given as shown in Eq. (4). Hence, from Equations (3) and (4), the corresponding path loss at a distance $d$ km from the transmitter is given by Eq. (5). Correspondingly, the calculated path loss in the suburban and urban areas, compared with free space loss is as shown in Figure 7. Here, it is observed that the pathloss for the urban setting is higher than the suburban setting for about 80% of the measurements period. This is expected because pathloss in suburban area is supposed to be less compared with pathloss in the urban area.

$$EIRP = 58.75\ dB + (-22.5)\ dBm = 36.25 dBm \quad (4)$$

$$PL = 36.25 dBm - P_R \quad (5)$$

**Table 2**. Base stations (eNodeBs) downlink parameters

| Parameters | Values |
|---|---|
| Maximum Transmitter Power | 43dBm |
| Multi-Antenna Combining Gain | 3dB |
| Transmitter Antenna Gain | 17dBi |
| Radio Frequency Filter + Cable Loss | 3dB |
| Pilot Power Boosting | 3dB |
| Transmitter Duplexing Loss | 0dB |
| Loss Due to Pilot Powers | -1.25dB |
| Total Transmit EIRP | 58.75dBm |
| Handoff Gain | 2.5dB |
| HARQ Gain | 3dB |
| Coding Gain | 0dB |
| Interference Margin | 2dB |
| Penetration Loss | 20dB |
| Log normal Fading Margin | 6dB |
| Other Losses and Gains | -22.5dB |

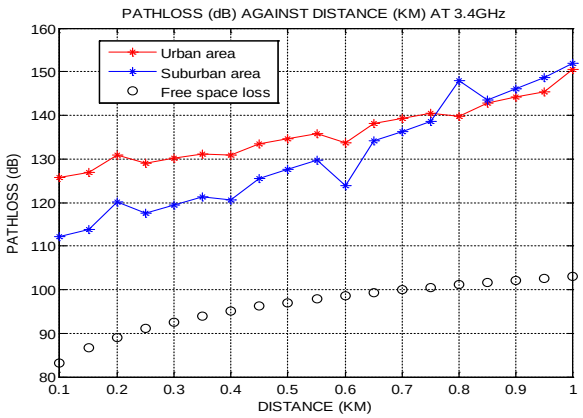


**Figure 7.** Comparison of path loss of measured data in suburban and urban areas

### 5.1 Results - Typical of a Suburban Area

The mobile receiver height was maintained at 1.5m, Tx-Rx distance increases in steps of 50m from 100m to 1.0km and a transmitter antenna height of 20m was used. Results typical of a suburban area are as shown in Fig. 8. Here, the predicted and the measured path loss vary logarithmically with propagation distance. It can be seen from Figure 8 that the SUI and the COST 231/WI models showed alarming deviations from the measured path loss. On the other hand, the Ericsson model showed the best match to measured data whereas the COST 231-Hata and ECC-33 models show close agreement with measured data.

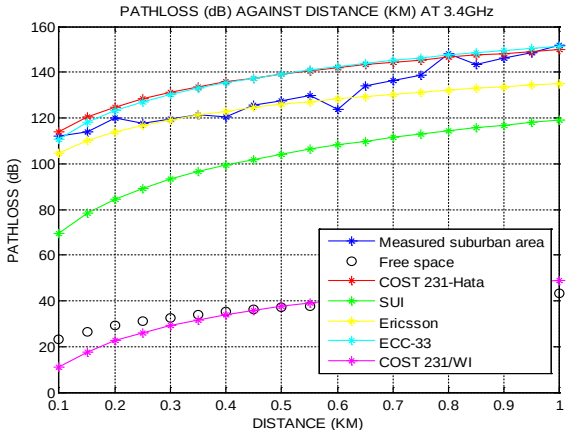


**Figure 8.** Predicted and measured pathloss in a suburban area

### 5.2 Results - Typical of an Urban Area

In the urban area, the operating frequency was set at 3400 MHz, the transmitter height at 24 m, transmitter (Tx)-receiver (Rx) distance was varied between 0.1km to 1.0km in steps of 50m at a near constant receiver antenna height of 1.5m. Variations in the predicted and measured path loss values are as shown in Figure 9. It shows that the COST-231 Hata model is the best fit to measured pathloss, and the Ericsson model show close relationship

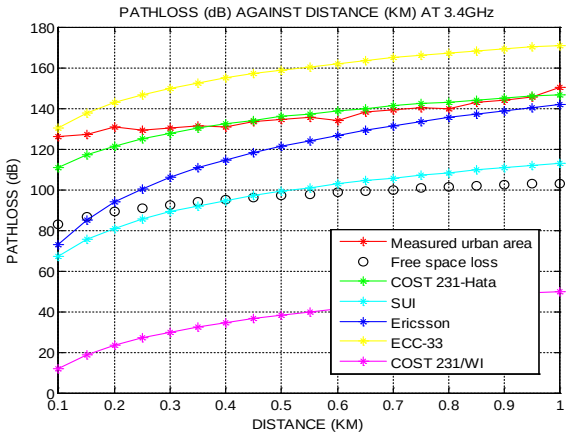


**Figure 9.** Predicted and measured path loss in an urban area

with the measured data, while the COST 231 Walfisch Ikegami (COST-231/WI), SUI and the ECC-33 models showed reasonable deviations from the measured data.

### 5.3 Root Mean Squared Error Analysis

The root-mean-squared error (RMSE) is used for error estimation between measured data and referenced or standardised data set. The RMSE represents the mean standard deviation between the measured and predicted values (Chebil et al., 2011; Ajose and Imoize, 2013).

$$RMSE = \sqrt{\sum_{i=1}^{n} \frac{\left(PL_{M,i} - PL_{P,i}\right)^2}{N}} \quad (6)$$

Where,

$PL_{M,i}$ is the actual sample values
$PL_{P,i}$ is the predicted sample values
$N$ is the number of data points

From Eq. (6), the RMSE for the measured and predicted path loss is given as shown in Eq. (7);

$$RMSE = \sqrt{\sum_{i=1}^{n} \frac{\left(PL_{measured,i} - PL_{predicted,i}\right)^2}{N}} \quad (7)$$

where

$PL_{measued,i}$ = Path loss of measured data in dB
$PL_{predicted,i}$ = Predicted path loss measured in dB
$N$ = 19 depicting the number of measured data points

The RMSE values follows directly from Eq. (7) with the resulting values for the suburban and urban areas are as shown in Table 3.

**Table 3.** Root mean squared errors in suburban and urban areas

| Pathloss models | Root mean squared errors (dB) | |
|---|---|---|
| | Suburban area | Urban area |
| Free Space | 34.9108 | 39.6194 |
| COST 231 Hata | 9.9103 | 5.1343 |
| SUI | 57.3672 | 48.4570 |
| Ericsson | 7.0797 | 15.1728 |
| ECC -33 | 8.6927 | 18.9087 |
| COST 231 W/I | 13.8730 | 5.2496 |

### 5.4 Best Model Selection

Measured pathloss at 3400 MHz in Ajah and Lagos-highland areas of Lagos State, Nigeria have been compared against predicted path loss. From Table 3, the minimum value of the RMSE observed is 5.1343dB in the urban area. This corresponds to the RMSE of the predicted pathloss for the COST-231-Hata model. The COST-231-Hata model, which satisfied the RMSE closest to zero, is taken as the best candidate for predicting the pathloss in the urban area.

Similarly, the minimum value of the RMSE as observed from Table 3 is 7.0797dB, for the suburban area. This corresponds to the RMSE of the pathloss predicted for the Ericsson model. Hence, the Ericsson model is the most suitable model for predicting the pathloss of measured data in the suburban area.

### 5.5 Modification of Selected Model for Urban Areas

The COST-231 Hata model has been selected as the best candidate for path loss prediction in the urban area. This is because it gives the best prediction (a value closest to zero) when compared with other contending models. However, there is a need to modify the model to improve its prediction accuracy. A modification of the COST 231 model can be achieved by adding the value of the corresponding RMSE to the model (Ajose and Imoize, 2013; Ogbeide and Edeko, 2013; Famoriji and Olasoji, 2013).

$$PL = 46.3 + 33.9.\log_{10} f - 13.82.\log_{10} h_b - 3.20[\log_{10}(11.75\, h_r)]^2 - 4.97 + [44.9 - 6.55.\log_{10} h_b].\log_{10} d + C_m \quad (8)$$

where,
$f_c$ = 3400MHz; $h_b$ = 24m
$h_r$ =1.5m; $C_m$ = 3 dB for urban
$d$ = distance between transmitter and receiver in meters

Adding the value of RMSE to Eq. (8) results in Eq. (9) in terms of $d$.

$$PL = 46.3 + 33.9.\log_{10}(3400) - 13.82.\log_{10}(24) - 3.20[\log_{10}(11.75 * 1.5)]^2 - 4.97 + [44.9 - 6.55.\log_{10} 20].\log_{10} d + 3 + RMSE \quad (9)$$

Here, it should be noted that the modification is aimed at giving better performance to the model, when compared to the actual predicted pathloss, hence the sign of the RMSE is important. By applying Eq. (7) in Eq. (9), we have;

$$PL = 46.3 + 33.9.\log_{10}(3400) - 13.82.\log_{10}(24) - 3.20[\log_{10}(11.75 * 1.5)]^2 - 4.97 + [44.9 - 6.55.\log_{10} 20].\log_{10} d + 3 + (-5.1343) \quad (10)$$

$$PL = 145.929 + 36.38.\log_{10}(d) \quad (11)$$

where $d$ = 0.1, 0.15, 0.2 … 1.0 *km*

Equation (11) shows a simplified and modified COST-231 Hata model for the selected urban area at 3400 MHz. The comparison of the measured pathloss, modified and predicted COST 231 Hata model is as shown in Figure 10.

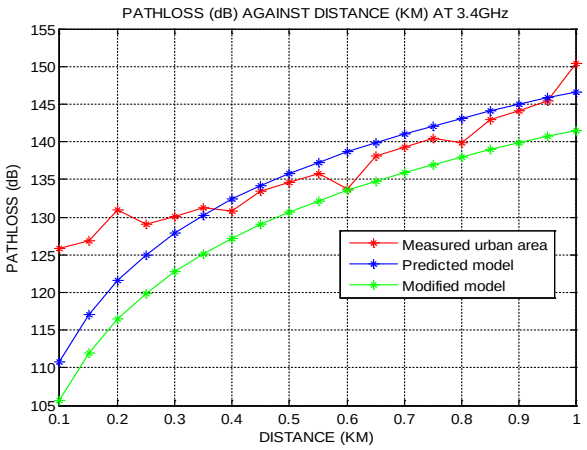


**Figure 10.** Comparison of measured pathloss, modified and predicted COST 231 Hata model for urban areas

### 5.6 Modification of Selected Model for Suburban Areas

The Ericsson model gives the best prediction in relation to the measured path loss in the suburban area, with an RMSE of 7.0797dB. The modification to the Ericsson model can be achieved by adding the value of the corresponding RMSE (± 7.0797dB). The Ericsson model is given (Ibhaze et al., 2017) as shown in Eq. (12).

$$PL = a_0 + a_1.\log_{10}(d) + a_2.\log_{10}(h_b) + a_3.\log_{10}(h_b)\log_{10}(d) - 3.2(\log_{10}(11.75h_r))^2) + g(f) \quad (12)$$

$$PL = 36.2 + 30 * \log_{10}(d) + 12 * \log_{10}(20) + 0.1 * \log_{10}(20)\log_{10}(d) - 3.2 * (\log_{10}(11.75 * 1.5))^2) + 44.49 * \log_{10} 3400 - 4.78 * (\log_{10} 3400)^2 + RMSE \quad (13)$$

Applying Eq. (7) in Eq. (13), gives;

$$PL = 36.2 + 30 * \log_{10}(d) + 12 * \log_{10}(20) + 0.1 * \log_{10}(20)\log_{10}(d) - 3.2 * (\log_{10}(11.75 * 1.5))^2) + 44.49 * \log_{10} 3400 - 4.78 * (\log_{10} 3400)^2 + (-7.0797) \quad (14)$$

$$PL = 137.2683 + 30.33.\log_{10}(d) \quad (15)$$

where, $d$ = 0.1, 0.15, 0.2 … 1.0 *km*

The results showing a comparison of the measured pathloss, predicted and modified Ericsson model is as shown in Figure 11.

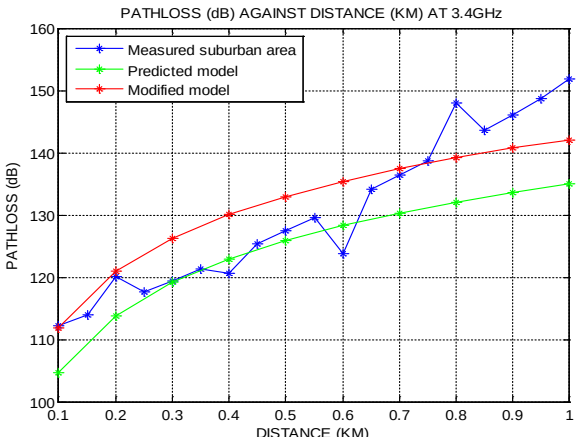


**Figure 11.** Comparison of the measured pathloss, modified and predicted Ericsson model for suburban areas

### 5.7 Development of Best Curve for Measured Pathloss

The least square regression method is generally adopted to fit a straight line or a curve to a set of data points (Hoffman and Frankel, 2001; Hamming, 2012; Stroud, and Booth, 2013). A second order polynomial of the form $y = a + bx + cx^2$ has been chosen to fit the measured path loss data. Generally for a $j^{th}$ order polynomial of the form of Eq. (16) (Stroud and Booth, 2013);

$$f(x) = a_j x^j + a_{j-1} x^{j-1} + a_{j-2} x^{j-2} + \ldots + a_0 \quad (16)$$

Polynomial equations of the best fit are given as;

$$a_0 N + a_1 \sum x_i + \ldots + a_j \sum x_i^{\,j} = \sum x_i f(x)_i \quad (17)$$

$$a_0 \sum x_i + a_1 \sum x_i^{\,2} + \ldots + a_j \sum x_i^{\,j+1} = \sum x_i^{\,2} f(x)_i \quad (18)$$

$$\vdots \qquad \vdots \qquad \vdots \qquad \vdots$$

$$a_0 \sum x_i^{\,j} + a_j \sum x_i^{\,j+1} + \ldots + a_1 \sum x_i^{\,2j} = \sum x_i^{\,j} f(x)_i \quad (19)$$

where

$N$ = number of data points

$i$ = position of each of the data points

$j$ = order of the polynomial

Equations (17) – (19) can be written in matrix form as shown in Eq. (20).

$$\begin{bmatrix} n & \sum x_i & \ldots & \sum x_i^{\,j} \\ \sum x_i & \sum x_i^{\,2} & \ldots & \sum x_i^{\,j+1} \\ \vdots & \vdots & \vdots & \vdots \\ \sum x_i^{\,j} & \sum x_i^{\,j+1} & \ldots & \sum x_i^{\,2j} \end{bmatrix} \begin{bmatrix} a_0 \\ a_1 \\ \vdots \\ a_j \end{bmatrix} = \begin{bmatrix} \sum x_i f(x)_i \\ \sum x_i^{\,2} f(x)_i \\ \vdots \\ \sum x_i^{\,j} f(x)_i \end{bmatrix} \quad (20)$$

In terms of the path loss of measured data $PL_{measured}$ and the distance between the transmitting and the receiving antennas, Eq. (20) can be re-written as in Eq. (21);

$$\begin{bmatrix} n & \sum d_i & \ldots & \sum d_i^{\,j} \\ \sum d_i & \sum d_i^{\,2} & \ldots & \sum d_i^{\,j+1} \\ \vdots & \vdots & \vdots & \vdots \\ \sum d_i^{\,j} & \sum d_i^{\,j+1} & \ldots & \sum d_i^{\,2j} \end{bmatrix} \begin{bmatrix} a_0 \\ a_1 \\ \vdots \\ a_j \end{bmatrix} = \begin{bmatrix} \sum d_i PL_{measured,i} \\ \sum d_i^{\,2} PL_{measured,i} \\ \vdots \\ \sum d_i^{\,j} PL_{measured,i} \end{bmatrix} \quad (21)$$

A resultant second order polynomial in terms of the fitted values for the measured path loss $PL_{fitted}$ and the distance $d$ is of the form of Eq. (22);

$$PL_{fitted} = a + b * d + c * d^2 \quad (22)$$

Comparing Eq. (16) to Eq. (22), $a_0 = a$, $a_1 = b$, $a_2 = c$. The least square regression data for measured path loss in the suburban and urban areas are as shown in Table 4, and Eq. (23) follows directly from Eq. (21) and Table 4.

**Table 4.** Least square regression data for measured path loss in suburban and urban areas

| Parameters | Suburban Area | Urban Area |
|---|---|---|
| $d$ | 10.45 | 10.45 |
| $d^2$ | 7.1725 | 7.1725 |
| $D^2$ | 5.1524 | 5.1524 |
| $d^4$ | 4.5169 | 4.5169 |
| $PL_{measured}$ | 2478.8 | 2582.6 |
| $d * PL_{measured}$ | 1425.6 | 1453.7 |
| $d^2 * PL_{measured}$ | 1006.1 | 1012.8 |

$$\begin{bmatrix} 19 & 10.45 & 7.1725 \\ 10.45 & 7.1725 & 5.1524 \\ 7.1725 & 5.1524 & 4.5169 \end{bmatrix} \begin{bmatrix} a \\ b \\ c \end{bmatrix} = \begin{bmatrix} 2582.6 \\ 1453.7 \\ 1012.8 \end{bmatrix} \quad (23)$$

As shown in Eq. (23), the constants a, b and c are solved using a third order determinant method in MATLAB (Hoffman and Frankel, 2001). The results are highlighted as shown in Eq. (24);

$$a = 126.2429,\ b = 8.0496,\ c = 13.9272 \quad (24)$$

Now, we substitute the values in Eq. (24) into Eq. (22), resulting in the curve that best fit the measured data in the urban area as shown in Eq. (25);

$$PL_{fitted} = 126.2429 + 8.0496d + 13.9272d^2 \quad (25)$$

Similarly, we derive a suitable equation for the suburban area, following the same approach for the urban area. From Table 4, and applying Eq. (21), the values of a, b and c are computed for the suburban area by solving Eq. (26);

$$\begin{bmatrix} 23 & 10.45 & 7.1725 \\ 10.45 & 7.1725 & 5.1524 \\ 7.1725 & 5.1524 & 4.5169 \end{bmatrix} \begin{bmatrix} a \\ b \\ c \end{bmatrix} = \begin{bmatrix} 2478.8 \\ 1425.6 \\ 1006.1 \end{bmatrix} \quad (26)$$

Similar to Eq. (24), the values of a, b, and c are as shown in Eq. (27);

$$a = 111.1971,\ b = 20.5984,\ c = 21.0234 \quad (27)$$

The equation of the curve that best fit the measured path loss in the suburban area is given in Eq. (28).

$$PL_{fitted} = 111.1971 + 20.5984d + 21.0234d^2 \quad (28)$$

The comparison of the fitted data for the urban and suburban areas is as shown in Figures 12 and 13, respectively. The results depicted in Fig. 12 and Fig. 13 show that the least square (LS) curve fitting, approximately fits the measured data points with smaller error bound.

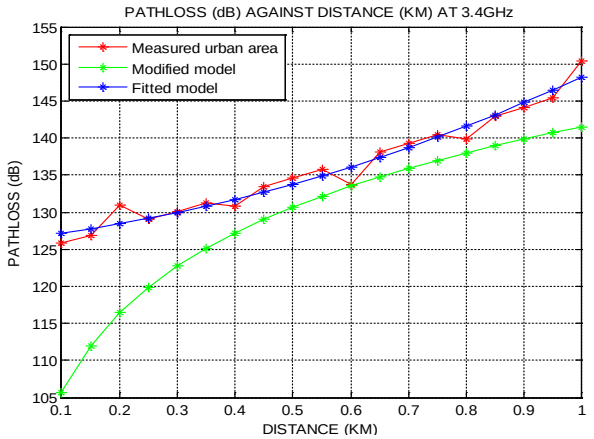


**Figure 12.** Comparison of measured pathloss, modified and fitted models for urban areas

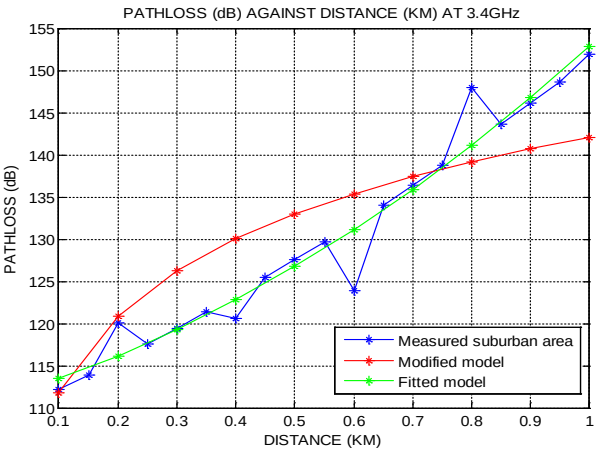


**Figure 13.** Comparison of measured pathloss, modified and fitted models for suburban areas

### 5.8 Validation of Models

In order to test the validity of the developed models for applicability in related environments, the RMSE analysis have been used to determine the error ratio based on the developed COST 231 Hata and the Ericsson models for urban and suburban areas, respectively. Applying Eq. (7), the results of the RMSE values are given as 6.20dB and 5.90dB for urban and suburban areas, respectively.

The developed models are found suitable for the investigated areas. This is because the RMSEs between the fitted, measured and predicted path loss values fall reasonably in the acceptable range of up to 6dB (Wu and Yuan, 1998; Ajose and Imoize, 2013; Ogbeide and Edeko, 2013; Famoriji and Olasoji, 2013, Popoola et al., 2018). However, the excess pathloss of 0.20dB observed for the urban area may be due to other dynamic factors such as high-density vehicular movements.

## 6. Conclusion

Path loss of propagation measurements taken from four eNodeBs of a 4G LTE network in the suburban and urban areas of Ajah and Lagos highlands in Lagos State, Nigeria, have been compared against well-known empirical models. Results revealed that the COST-231 Hata model outperformed other contending models in the urban area with an RMSE value of 5.13dB, and the Ericsson model showed the best performance in the tested suburban area, with an RMSE value of 7.08dB.

These models were selected and developed for the urban and suburban areas, respectively. The development was necessary to further reduce the RMSEs for improved path loss prediction in the areas. The developed models showed improved RMSEs values within the acceptable range of up to 6dB. Overall, the results compare favourably with related works reported for similar areas, and future work will focus on providing correction factors to ease the applicability of the models to other environments.

## References:


Abhayawardhana, V. S., Wassell, I. J., Crosby, D., Sellars, M. P., and Brown, M. G. (2005), "Comparison of empirical propagation path loss models for fixed wireless access systems", *Proceedings of the IEEE 61st Vehicular Technology Conference*, VTC 2005-Spring, Stockholm, Sweden, Vol. 1, May, pp. 73-77.

Ajose, S. O., and Imoize, A. L. (2013), "Propagation measurements and modelling at 1800 MHz in Lagos Nigeria", *International Journal of Wireless and Mobile Computing*, Vol.6, No.2, pp.165-174.

Athanasiadou, G. E. (2009), "Fixed wireless access propagation modelling and measurements", *Proceedings of the IEEE 69th Vehicular Technology Conference*, VTC Spring 2009, Barcelona, Spain, April, pp. 1-5.

Aragon-Zavala, A. (2008), *Antennas and Propagation for Wireless Communication Systems*, John Wiley and Sons.

Bola, G. S., and Saini, G. S. (2013), "Path loss measurement and estimation using different empirical models for WiMAX in urban area", *International Journal of Scientific and Engineering Research*, Vol.4, No.5, pp.1421-1428.

Chebil, J., Lawas, A. K., and Islam, M. D. (2013), "Comparison between measured and predicted path loss for mobile communication in Malaysia", *World Applied Sciences Journal 21 (Mathematical Applications in Engineering)*, pp. 123-128.

Chebil, J., Lwas, A. K., Islam, M. R., and Zyoud, A. H. (2011), "Comparison of empirical propagation path loss models for mobile communications in the suburban area of Kuala Lumpur", *Proceedings of the IEEE 2011 4th International Conference on Mechatronics (ICOM)*, Kuala Lumpur, Malaysia, May, pp. 1-5.

Dahlman, E., Parkvall, S., and Skold, J. (2013), *4G: LTE/LTE-Advanced for Mobile Broadband*, Academic Press.

Dimou, K., Wang, M., Yang, Y., Kazmi, M., Larmo, A., Pettersson, J. and Timner, Y. (2009), "Handover within 3GPP LTE: design principles and performance", *Proceedings of the IEEE 70th Vehicular Technology Conference* (VTC 2009-Fall), Anchorage, Alaska, USA, September, pp. 1-5.

ElNashar, A., El-Saidny, M. A., and Sherif, M. (2014), *Design, Deployment and Performance of 4G-LTE Networks: A Practical Approach*, John Wiley and Sons.

Famoriji, J. O., and Olasoji, Y. O. (2013), "UHF radio frequency propagation model for Akure metropolis", *Research Journal of Engineering Sciences*, Vol. 2(5), May, pp.6-10.

Hamming, R. (2012), *Numerical Methods for Scientists and Engineers*, Courier Corporation.

Hoffman, J. D., and Frankel, S. (2001), *Numerical Methods for Engineers and Scientists*, CRC press.

Holma, H., and Toskala, A. (2007) (Eds.), *HSDPA/HSUPA for UMTS: High-speed Radio Access for Mobile Communications*, John Wiley and Sons.

Ibhaze, A. E., Ajose, S. O., Atayero, A. A., and Idachaba, F. E. (2016), "Developing smart cities through optimal wireless mobile network", *Proceedings of the IEEE International Conference on Emerging Technologies and Innovative Business Practices for the Transformation of Societies (EmergiTech)*, Balaclava, Mauritius, August, pp. 118-123.

Ibhaze, A. E., Imoize, A. L., Ajose, S. O., John, S. N., Ndujiuba, C. U., and Idachaba, F. E. (2017), "An empirical propagation model for path loss prediction at 2100 MHz in a dense urban environment", *Indian Journal of Science and Technology*, Vol.8, No.1, pp. 1-9.

Kale, S. S., and Jadhav, A. N. (2013), "Performance analysis of empirical propagation models for WiMAX in urban environment", *IOSR Journal of Electronics and Communication Engineering (IOSR-JECE)*, Vol.3, No.5, pp. 24-28.

Kamboj, V., Gupta, D. K., and Birla, N. I. (2011), "Comparison of path loss models for WiMAX in rural environment at 3.5 GHz", *International Journal of Engineering Science and Technology (IJEST)*, Vol.3, No.2, pp.1432-1437.

Katev, P. D. (2012), "Propagation models for WiMAX at 3.5 GHz", *Proceedings of the IEEE 9th International Conference – 2012 ELEKTRO*, Rajeck Teplice, Slovakia, May pp.61-65. DOI: 10.1109/ELEKTRO.2012.6225572

Khan, I., Eng, T. C., and Kamboh, S. A. (2012), "Performance analysis of various path loss models for wireless network in different environments", *International Journal of Engineering and Advanced Technology (IJEAT)*, Vol. 2, No.1, October, pp. 161-165.

Korowajczuk, L. (2011), *LTE, WiMAX and WLAN Network Design, Optimisation and Performance Analysis*, John Wiley and Sons.

Milanovic, J., Rimac-Drlje, S., and Bejuk, K. (2007), "Comparison of propagation models accuracy for WiMAX on 3.5 GHz", *Proceedings of the 14th IEEE International Conference on Electronics, Circuits and Systems, ICECS 2007*, Marrakech, Morocco, December, pp. 111-114.

Mishra, A. R. (2004), *Fundamentals of Cellular Network Planning and Optimisation: 2G/2.5 G/3G Evolution to 4G*, John Wiley and Sons.

Molisch, A. F. (2012), *Wireless Communications*, Vol.34, John Wiley and Sons.

Mollel, M. S., and Kisangiri, M. (2014), "Comparison of empirical propagation path loss models for mobile communication", *Computer Engineering and Intelligent Systems*, Vol.5, No.9, pp. 1-10.

Ogbeide, O. K., and Edeko, F. O. (2013), "Modification of the Hata empirical propagation model for application in VHF band in Edo State, Nigeria", *International Journal of Engineering Science Invention*, Vol.2, No.8, pp. 35-39.

Podder, P. K., Islam, F., Sarker, D. K., Hasan, M. G., and Kundu, D. (2012), "An analytical study for the performance analysis of propagation models in WiMAX", *International Journal of Computational Engineering Research*, Vol.2, pp.175-181.

Popoola, S. I., Adetiba, E., Atayero, A. A., Faruk, N., and Calafate, C. T. (2018), "Optimal model for path loss predictions using feed-forward neural networks", *Cogent Engineering*, Vol.5, No.1, 1444345. https://doi.org/10.1080/23311916.2018.1444345

Ramiro, J., and Hamied, K. (2011) (Eds), *Self-organising Networks (SON): Self-planning, Self-optimisation and Self-healing for GSM, UMTS and LTE*, John Wiley and Sons.

Rappaport, T. S. (1996), *Wireless Communications: Principles and Practice*, Vol. 2. Prentice Hall, New Jersey

Sesia, S., Baker, M., and Toufik, I. (2011), *LTE-the UMTS Long Term Evolution: From Theory to Practice*, John Wiley and Sons.

Shabbir, N., Sadiq, M. T., Kashif, H., and Ullah, R. (2011). "Comparison of radio propagation models for long-term evolution (LTE) network", *International Journal of Next-Generation Networks (IJNGN)*, vol.3, No.3, pp. 27-41.

Song, L., and Shen, J. (2010) (Eds.), *Evolved Cellular Network Planning and Optimisation for UMTS and LTE*, CRC Press.

Stroud, K. A., and Booth, D. J. (2013), *Engineering Mathematics*, Palgrave Macmillan.

Wu, J., and Yuan, D. (1998), "Propagation measurements and modeling in Jinan city", *Proceedings of the 9th IEEE International Symposium on Personal, Indoor and Mobile Radio Communications*, Boston, Massachusetts, USA, Vol. 3, September, pp. 1157-1160.

## Authors' Biographical Notes:

Agbotiname Lucky Imoize *is a Lecturer in the Department of Electrical and Electronics Engineering, University of Lagos, Nigeria, and presently a Fulbright Visiting Research Scholar with the Wireless at Virginia Tech Labs, Bradley Department of Electrical and Computer Engineering, Virginia Polytechnic Institute and State University, Virginia USA. He received his BEng (Hons) in Electrical and Electronics Engineering from Ambrose Alli University, Ekpoma, Nigeria, in 2008, and MSc in Electrical and Electronics Engineering with specialisation in Communications Engineering from University of Lagos, Nigeria, in 2012. He was elected as a Corporate Member of the Nigerian Society of Engineers, and he is a registered Engineer with the Council for the Regulation of Engineering in Nigeria (COREN). His research interests are in the areas of propagation measurements, channel modeling and multi-channel communications.*

Augustus Ehiremen Ibhaze *is presently a Lecturer in the Department of Electrical and Electronics Engineering, University of Lagos, Nigeria. He holds an M.Sc in Electrical and Electronics Engineering from the University of Lagos (2012) and B.Eng (Hons) in Electrical Engineering from Ambrose Alli University, Ekpoma, Nigeria, in 2008. He holds a Professional Certification in Information Technology service management (ITILversion3), Netherlands. He was elected as a Corporate Member of the Nigerian Society of Engineers and he is a registered Engineer with the Council for the Regulation of Engineering in Nigeria (COREN).*

Peace Oluchukwu Nwosu *is presently a practicing Engineer in Lagos, Nigeria. She completed Masters of Science in Electrical and Electronics Engineering, with specialisation in Communications Engineering at the University of Lagos, Akoka, Lagos, in 2012. Her current research interest is in the area of wireless communications engineering.*

Simeon Olumide Ajose *is a Professor of Electronics and Computer Engineering in Lagos State University. He was the Dean of Engineering from 1998 to 2002. He holds a BSc (Hons) in Electrical Engineering from the University of Lagos, Nigeria (1971), MSc and PhD from the University of London King's College in 1974 and 1976, respectively. He became a Fellow of the Nigerian Society of Engineers (FNSE) in 1989 and was featured in the first issue of International Who's Who in Engineering. His research interests are in the areas of microwave networks, digital signal processing and communication technology.*

■

**ISSN 0511-5728**
*The West Indian Journal of Engineering*
Vol.41, No.2, January 2019, pp.22-30

# Modular and 3D-Design of a Fluidised Bed Boiler with Agricultural Residue for Steam Energy Production

Muyideen B. Balogun[a,Ψ], Clement O. Folayan[b], Dangana M. Kulla[c], Fatai O. Anafi[d], Samaila. Umaru[e] and Nua O. Omisanya[f,g]

[a,b,c,d,e,f] Department of Mechanical Engineering, Ahmadu Bello University, P.M.B 1045, Zaria, Kaduna State Nigeria;
[g]National Automotive Design and Development Council, P.M.B 320, Garki, Abuja, Nigeria;

[a]E-mail: balo.muyi@gmail.com;
[b]E-mail: clementfolayan@yahoo.com;
[c]E-mail: dmkulla2@yahoo.com;
[d]E-mail: fataianafi@yahoo.com;
[e]E-mail: bnumar@yahoo.com;
[f,g]E-mail: ominua@yahoo.com

[Ψ] *Corresponding Author*

*(Received 18 February 2018; Revised 23 April 2018; Accepted 13 September 2018)*

**Abstract:** *In this study, a miniature fluidised bed boiler for steam generation was designed and constructed. The boiler is made up of a steam drum, combustion chamber, downcomer and riser tubes as a heat exchanger, a non-return valve and superheater tube. Experimental investigation on the fuel distribution was carried in two-dimensional chamber with cross-section of 500 mm x 1000 mm and bed height of 77 mm, 47 mm and 27 mm. The results obtained from the performance evaluation of the fluidised bed boiler operated with corncob at constant feed rate of 6kg/h for various bed heights of 77 mm, 47 mm and 27 mm recorded stability in the saturation temperature of 121 $^oC$ at 50 minutes, 144 $^oC$ at 45 minutes and 153 $^oC$ at 30 minutes, respectively. In additional, saturation pressures of 2.0 bar from 50 to 55 minutes for bed height of 77 mm, 2.1 bar from 45 to 50 minutes for bed height of 47 mm and 3.6 to 3.7 bar from 45 to 55 minutes for bed height 27 mm were obtained. The effect of fuel particle size on emissions and over all combustion efficiency of corncobs has proven to be efficient in a fluidised bed boiler as the emission analysis of the flue gas has shown to be low in various percentages of 0.0003% of $NO_x$, 0.001% HC, 0.02% of CO and 0.93% of Nitrogenm, respectively.*

***Keywords:*** *Solid fuels, Bed height, Heat transfer, Steam, Saturated temperature, Saturated pressure, Flue gas*

## 1. Introduction

Fluidised bed combustion (FBC) is a combustion technology that offers many unique advantages such as large interfacial surface areas between the fluid (gas or liquid) and particles, high fluid-particles contact efficiency, excellent heat transfer, uniform bed temperature and the ability to handle wide range of solid fuels (Thenmozhi and Sivakumar, 2013; Zhou et al., 2008). In its most basic form, fuel particles are suspended in a hot, bubbling fluidity bed of ash and other particulate materials (sand, limestone, etc.) through which jets of air are blown to provide the oxygen required for combustion. The resultant fast and intimate mixing of gas and solids promotes rapid heat transfer and chemical reactions within the bed. FBC plants are capable of burning a variety of low-grade solid fuels, including most types of coal and woody biomass, (Thenmozhi and Sivakumar, 2013) at high efficiency and without the necessity for expensive fuel preparation (e.g., pulverising).

According to American Society of Mechanical Engineers (ASME), a steam generating unit is defined as a combination of apparatus for producing, furnishing or recovering heat together with the apparatus for transferring the heat so made available to the fluid being heated and vaporised (Rajput, 2010). Boilers are pressure vessels designed to heat water or produce steam, by combustion of fuel which can then be used to provide space heating and/or service water heating to a building (Odigure et al., 2005). Steam is preferred over hot water in some applications, including absorption cooling, kitchens, laundries, sterilisers, and steam driven equipment. Steam is therefore important in engineering and energy studies. Boilers are classified into different types based on their working pressure and temperature, fuel type, draft method, size and capacity, and whether they condense the water vapour in the combustion gases.

Boilers are also sometimes described by their key components, such as heat exchanger materials or tube design. Two primary classifications of boilers are Fire tube and Water tube boilers. In a Fire tube boiler, hot gases of combustion flow through a series of tubes surrounded by water. On the other hand, in a water tube boiler, water flows in the inside of the tubes and the hot gases from combustion flow around the outside of the tubes. Steam generator is a complex integration of

furnace, superheater, reheater, boiler or evaporator, economiser and air preheater, along with various auxiliaries such as pulverises, burners, fans, stokers, dust collectors and precipitators, ash-handling equipment, and chimney or stack. The boiler (or evaporator) is that part of the steam generator where phase change (or boiling) occurs from liquid (water) to vapour (steam), essentially at constant pressure and temperature (Nag, 2008).

Biomass is an intriguing alternative fuel as it is readily available in various forms throughout the world, is renewable and can be harnessed by agricultural means. Though biomass is a renewable source, the growth of some materials, such as wood, is a very long process and cannot be rapidly grown, while other crops are perennial, such as corn, straw and switch grass (Saidur et al., 2011). Growth rate as well as availability must be considered while selecting a viable crop. It is also necessary to replace nutrients that are absorbed from the ground by plant growth or biomass production will be depleted over time (Christensen, 2011).

A wide variety of techniquesis available to utilise biomass resources, but the most efficient have been to burn them directly for heat in a controlled environment. The crop residues that are commonly used as sources of energy includes rice husks, sugar cane fiber, groundnut shells, maize cobs, coconut husks, and palm oil fibre. (Kyauta et al., 2015). The use of biomass as alternative sources of energy is attractive because it addresses both problems of waste disposal and fuel wood shortages (Armesto et al., 2002; Varol et al., 2014). The extraction of useful energy from biomass could contribute to sustainable development and bring very significant social and economic benefits to both rural and urban areas (Khan et al., 2009). Folayan et al. (2015) investigated the environmentally friendly methods of extracting biomass energy for rural use, one such means is energy recovery using fluidised bed combustors. This system uses agricultural waste as fuel source to produce heat energy as an alternative to power rural community for light load applications. Test results recorded high flue gas and bed temperatures of over 300°C and 850°C respectively, suitable for rural application including grain drying and water boiling.

Martínez et al. (2011) presented the conceptual design of a three fluidised beds combustion system capturing $CO_2$ with CaO. In their work, three fluidised bed reactors are interconnected in such a way that it is possible to perform the $CaCO_3$ calcination at a temperature of 950 $^oC$ with the energy transported by a hot solid stream produced in the circulating fluidised bed combustor operating at 1030 $^oC$. They presented that the stream rich in CaO produced in the calciner was splited into three parts. The reported result shows that due to high temperatures involved in all the system, it was possible to recover most of the energy in the fuel and to produce power in a supercritical steam cycle. A case study was studied and it was demonstrated that under these operating conditions, 90% $CO_2$ capture efficiency can be achieved with no energy penalty further than the one originated in the $CO_2$ compression system.

Ohijeagbon et al. (2013) reported on the design of laboratory fire tube boiler for eventual construction and use as teaching aid and for research purposes, the design enables the availability of portable and affordable steam boiler for steam generation in school laboratory and to enhance research and students' learning process in area of thermodynamics, heat transfer and energy studies.

The objective of this work seeks the utilisation of locally sourced materials to design, develop and test the fluidised bed boiler for steam generation by carrying out technical feasibility of using corncob as fuel and varying the bed height while keeping the superficial velocity of fluidising gas constant. More so, the characteristic of the steam generated was used in the selection of an applicable steam turbine.

## 2.0 Material and Methods

### 2.1 Description of the Fluidised Bed Boiler

The physical geometry of the fluidised bed water tube boiler was developed and a 3-D model diagram is shown in Figure 1. The boiler consists fundamentally of the fluidised bed combustion chamber and steam drum, other parts such as; steam tubes, steam trap, steam tap, downcomer, exhaust pipe, air blower and insulations were designed in the geometry of the miniature water-tube steam boiler.

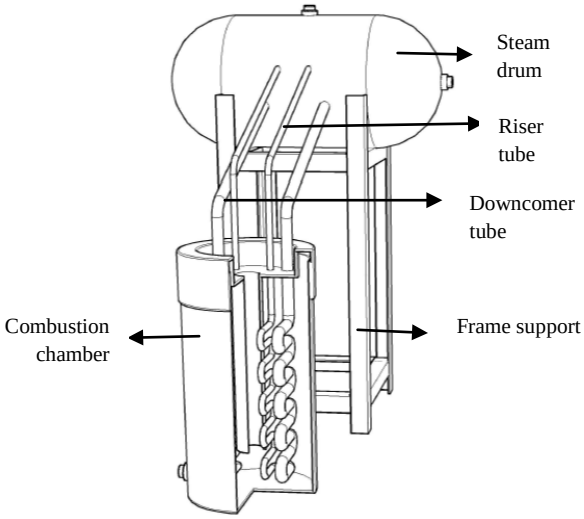


**Figure 1.** 3-D Model of the Developed Boiler

### 2.2 Design Considerations

The systematic approached to the design, fabrication, experimental procedure and testing of the (Boiler and Code, 1989) developed bubbling fluidised bed boiler for energy generation are as follows:

i. Steam pressure of 2 bar to 5 bar
ii. Steam temperature of 120 $^oC$ to 180 $^oC$
iii. Steam capacity of 2 kg/h to 10 kg/h

iv. Stoichiometric air-fuel ratio
v. Calorific value of corncob as fuel

### 2.3 Material Selection

The suitable materials selected for the fabrication of the fluidised bed boiler were selected based on the physical and mechanical properties, and their availability. The materials include the following:

i. Galvanised plate was used for the steam drum because it can withstand high temperature applications and resistivity to corrosion.
ii. Galvanised pipes were used for steam tubes due to its hollow shape.
iii. Mild steel plate was used for fluidised bed combustion chamber because of its high melting temperature resistance.
iv. Mild steel used as the grate and distributor plate because of the reaction that is expected to occur during combustion.
v. Safety valve and Non-return valve were made of brass
vi. Granular Material (Sand)
vii. Pipes and Fittings were made of galvanised materials

### 2.4 Design Theories and Calculations

The boiler is a vessel that operates under pressure; hence, the design theories are the basic principles considered to evaluate the various parameters, dimensions and the performance of the boiler under internal pressure.

#### 2.4.1 Internal Designed Pressure of a Boiler

The design pressure higher than operating pressure with 10% or more will satisfy the requirement. The maximum allowable working pressure is the maximum permissible pressure at the top of the boiler in its normal operating position at specific temperature. This pressure is based on the nominal thickness. The internal design pressure is given by (Ohijeagbon et al., 2013).

$$P_d = \frac{\sigma_u \times t}{R_i \times f_s} \quad (1)$$

where, $P_d$ = Internal design pressure on inside of drum or shell (N/m$^2$)
$\sigma_u$ = Ultimate strength of plate (N/m$^2$)
$t$ = Thickness of plate (m)
$R_i$ = Internal radius of drum (m)
$f_s$ = Factor of safety (ultimate strength divided by allowable working stress)

Tensile stress, $\sigma_{ut}$ = 385 MN/m$^2$

Compressive stress, $\sigma_{uc}$ = 665 MN/m$^2$

Shear stress, $\tau$ = 308 MN/m

#### 2.4.2 Stresses in Tubes and Drums

Stresses are induced in different parts of an operating boiler by the temperatures and pressures of hot flue gases, feed water and steam respectively. The magnitudes of these stresses must be known so that the boiler will be operated under safe conditions. Thus, the wall of the boiler subjected to internal pressure has to withstand two types of tensile stress, namely, 1) Circumferential or hoop stress and 2) Longitudinal stress (Khurmi and Gupta, 2005)

$$\sigma_{t1} = \frac{P_d \times D_i}{2t} \quad (2)$$

where, $P_d$ = Internal design pressure of the drum or shell (N/m$^2$)
$\sigma_{t1}$ = Circumferential or hoops stress (N/m$^2$)
$t$ = Thickness of plate (m)
$D_i$ = Internal diameter of drum (m)

$$\sigma_{t2} = \frac{P_d \times D_i}{4t} \quad (3)$$

where, $\sigma_{t2}$ = Longitudinal stress (N/m$^2$)

#### 2.4.3 Design of the Steam Drum

The design of this component must be strong enough to contain steam or hot water that was generated and to mechanically hold the boiler tubes as they expand and contract with changes in temperature. Hence, its volume is of importance and is written as (Balogun et al., 2016).

$$V_{dru} = A_{dru} \times L_{dru} \quad (4)$$

where, $A_{dru}$ = Cross sectional area of the drum (m$^2$)
$L_{dru}$ = Length of the drum (m)

#### 2.4.4 Design of the Steam Tube

Materials which can withstand high temperature and resistance to corrosion such as galvanised steel material was selected to form tubes.

$$V_{st} = A_{st} \times L_{st} \quad (5)$$

where, $A_{st}$ = Cross sectional area of the tube (m$^2$)
$L_{st}$ = Length of the drum (m)

#### 2.4.5 Design Height of the Combustion Chamber

This is given by the ratio of volume to combustion chamber area of the boiler (Balogun et al., 2016).

$$H_{com} = V_{com} / A_{com} \quad (6)$$

where, $H_{com}$ = Height of the combustion chamber (m)
$V_{com}$ = Volume of the combustion chamber (m$^3$)
$A_{com}$ = Cross sectional area of the combustion chamber (m$^2$)

#### 2.4.6 Minimum Wall Thickness of Tubes and Drum

The minimum required wall thickness of a boiler is a value beyond which the boiler wall cannot be easily damage by the operation pressure in a boiler. The formula is given as (Ohijeagbon et al., 2013).

$$t_w = \frac{P_d \times R_i}{\sigma \times \eta_E - 0.6P_d} \quad (7)$$

where, $\sigma$ = Allowable working stress of the material (N/m$^2$)

$t_w$ = Minimum wall thickness (m)

$\eta_E$ = Ligament efficiency of the welded joint

Therefore, the minimum wall thickness of the tubes is given as:

$$t_{w\,tubes} = \frac{P_d \times r_i}{2 \times \sigma \times \eta_E + 0.8P_d} + C \quad (8)$$

where, $C$ = Corrosion allowance

### 2.4.7 Velocity of Fluid inside Tubes, Pipes and Drum

To control the boiler operation, it is necessary to determine the velocity of fluid. It is given as (Ganapathy, 2003)

$$V = 0.05 \times M_w \times \frac{v}{D_i^2} \quad (9)$$

where, $V$ = Velocity (m/s)

$v$ = Specific volume of liquid (m$^3$/kg)

$M_w$ = Mass of water in the steam drum (kg/hr)

$D_i^2$ = Square of inner diameter of the drum (mm)

For steam, $v$ can be obtained from steam table.

### 2.4.8 Quantity Flow Rate of Fluid inside Tubes

The quantity of fluid to be delivered depends upon the inside diameter of the tube, and is given as:

$$Q_d = \frac{\pi}{4} d_i^2 \times V \quad (10)$$

where, $Q_d$ = Quantity flow rate (m$^3$/h)

Therefore, in boiler design the operating pressure of a boiler must be determined in order to make other important calculations required for effective functioning of the boiler. Table 1 shows the summary of the design calculation.

### 2.5 Construction Procedures

The techniques followed in order to achieve the modular construction of the developed fluidised bed water-tube boiler and evaluation of the materials that were used are as follows:

### 2.5.1 Combustion Chamber

The combustion chamber was fabricated from mild steel of thickness 3 mm, which was rolled into shape to form a diameter of 0.5 m and 1 m long (see Figure 2), was adopted for the fluidised bed combustion chamber. A perforated distributor grate that was made from mild steel was also adopted for the combustion of fuel and the whole combustion chamber was enhanced by air blower rated as 0.28 kW which provides the air for combustion.

### 2.5.2 Steam Drum

The steam drum was fabricated from a galvanised steel of 3 mm thick and welded together by gas welding to form the drum of 1m long and 0.6 m in diameter (see Figure 2), in which water was feed in at top through a valve, and steam tubes and downcomers was also be welded to it. The downcomer which convey water from the drum into combustion chamber where it was heated to form steam due to density differences of water in both steam tubes and downcomers results into natural circulation. Lastly, it was designed to hold up to 40 liters of water, steam pressure of 5 bars was also anticipated and steam capacity of 10 kg/h was also being desired.

**Figure 2.** Combustion Chamber at Early Stage of Fabrication with Coiling of Tubes

**Figure 3.** Steam Drum at Early Stage of Fabrication (Gas Welding)

### 2.5.3 Steam tubes

Materials which can withstand high temperature and resistance to corrosion such as galvanised steel materials were selected to form tubes. The steam tubes of 0.0127 m diameter were achieved after machining processes. Both downcomer and riser tubes were fabricated from a ¾" and ½" galvanised pipe of 3 m long that was cut and then bent it into 3" curvature (see Figure 3), which was 76.2 mm. Two (2) downcomer and riser tubes were achieved in line with these design specifications, welded to front of the steam drum, and went through the top of the combustion chamber. The curvature of tubes at the bottom bend was allowed to suspend at a height of 0.3 m just above the distributor plate.

**Table 1.** Summary of the Design Calculation

| Initial Data | Calculations | Results and Remarks |
|---|---|---|
| Type of boiler | Bubbling fluidised bed boiler | |
| **Internal designed pressure of the boiler** | | |
| $\sigma_{ut}$ = 385 MN/m$^2$<br>$t$ = 0.003 $m$<br>$R_i$ = 0.3 $m$<br>$f_s$ = 5 | $P_d = \frac{\sigma_u \times t}{R_i \times f_s} = \frac{385 \times 0.003}{0.3 \times 5}$<br>$P_d = 0.77\ MN/m^2 \cong 770{,}000\ N/m^2$<br>Hence, $P_d = 7.7\ bar$ | The design pressure was calculated as:<br>$P_d = 7.7\ bar$ |
| **Stresses in the tubes and drum** | | |
| For the Drum<br>$P_d$ = 7.7 $bar$<br>$t$ = 0.003 $m$<br>$D_i$ = 0.6 $m$ | $\sigma_{t1} = \frac{P_d \times D_i}{2t} = \frac{0.77 \times 0.6}{2 \times 0.003}$<br>$\sigma_{t1} = 77\ MN/m^2$<br>$\sigma_{t2} = \frac{P_d \times D_i}{4t} = \frac{0.77 \times 0.6}{4 \times 0.003}$<br>$\sigma_{t2} = 38.5\ MN/m^2$ | $\sigma_{t1}$ = Circumferential or hoops stress (N/m$^2$). Calculated as<br>$\sigma_{t1} = 77 \times 10^6\ N/m^2$<br>$\sigma_{t2}$ = Longitudinal stress (N/m$^2$). Calculated as<br>$\sigma_{t2} = 38.5 \times 10^6\ N/m^2$ |
| **Design of steam drum** | | |
| $D_i = 0.6\ m$<br>$L_{dru}$ = 1 $m$ | Volume of steam drum or boiler shell<br>$\frac{\pi}{4} \times 0.6^2 \times 1 = 0.283\ m^3$ | For this design specification, the volume of steam drum was calculated as<br>$V_{dru}$ = 0.283 $m^3$ |
| **Design of steam tubes** | | |
| $d_i = 0.0127\ m$<br>$L_{st}$ = 3 $m$ | Volume of tube<br>$\frac{\pi}{4} \times 0.0127^2 \times 3 = 0.038\ m^3$ | Babcock and Wilcox, stated that the minimum and maximum allowable tube diameter are 0.01 m and 0.0635 m. Therefore, the volume of the steam tube was calculated as<br>$V_{st}$ = $0.038\ m^3$ |
| **Design of combustion chamber** | | |
| $D_i = 0.5\ m$<br>$H_{com}$= 1 $m$ | Volume of combustion chamber<br>$V_{com} = \frac{\pi}{4} \times 0.5^2 \times 1 = 0.196\ m^3$ | For this design specification, the volume of combustion chamber was calculated as<br>$V_{com}$ = 0.196 $m^3$ |
| Types of feed<br>Bed material | Agricultural waste (chipped corncob and charcoal)<br>Sand | The corncob was from Shika community, Zaria.<br>Sand material of 250 µm and particle density of 2.659 $g/cm^3$ was used with bed height of 0.027 $m$, 0.047 $m$ and 0.77 $m$ were adopted. |
| **Design of minimum wall thickness** | | |
| For the Drum<br>$P_d = 0.77MN/m^2$<br>$D_i$ = 0.6 $m$<br>$\eta_E$ = 1<br>$\sigma_{t1} = 77\ MN/m^2$ | $t_w = \frac{P_d \times R_i}{\sigma \times \eta_E - 0.6P_d} = \frac{0.77 \times 0.3}{77 \times 1 - 0.6 \times 0.77}$<br>$t_w = 3.0181 \times 10^{-3}\ m$<br>$t_w = 3.018\ mm$ | $t_w = 3.018\ mm$<br>Take $t_w = 3.0\ mm$ |
| Also, for the tube<br>$d_i = 0.0127\ m$<br>$C = 3$ | $t_{w\ tubes} = \frac{P_d \times r_i}{2 \times \sigma \times \eta_E + 0.8P_d} + C$<br>$t_{w\ tubes} = \frac{0.77 \times 0.00635}{2 \times 77 \times 1 + 0.8 \times 0.77} + 3$<br>$t_{w\ tubes} = 3.0312\ mm$ | $t_{w\ tubes} = 3.0312\ mm$<br>Take $t_{w\ tubes} = 3.0\ mm$ |
| **Velocity of fluids in tubes, pipes and drum** | | |
| From steam table;<br>$v$ = 0.3427 $m^3/kg$ of water @ 155 $^oC$<br>$M_w$ = 48 kg/hr | $V = 0.05 \times M_w \times \frac{v}{D_i^2} = 0.05 \times 48 \times \frac{0.3427}{0.6^2}$<br>$V = 2.284\ m/s$ | For this design specification, the velocity of fluids in the steam drum is calculated to be<br>$V = 2.284\ m/s$ |
| **Quantity flow rate of fluid inside tubes** | | |
| $V = 2.284\ m/s$<br>$d_i$ = 0.0127 | $Q_d = \frac{\pi}{4} d_i^2 \times V = \frac{\pi}{4} \times 0.0127^2 \times 2.284$<br>$Q_d = 2.8933 \times 10^{-4}\ m^3/h$ | $Q_d$= 0.000289 m$^3$/h<br>$Q_d = 4.817 \times 10^{-6} m^3/min$ |
| **Design of frame support** | | |
| L = 0.6 $m$<br>B = 0.3 $m$<br>H = 1.5 $m$ | Area of frame support<br>$A_{fs} = 0.6 \times 0.3 \times 1.5 = 0.270\ m$ | $A_{fs} = 0.270\ m$ |

## 2.6 Experimental Procedure

Fine sand of 250 µm was fed evenly onto the distributor plate through the manhole opening up to a desired static bed height of 77 mm, 47 mm and 27 mm respectively. An air blower with capacity of 0.7 MPa rated 0.28 kW, 60 Hz was used to provide the buoyant forces for fluidisation and in addition provides the oxygen for combustion. Some charcoal in small pieces was fed onto the bed for pre-heating of the system. Additionally, 1 kg of the corncob waste samples from Shika community, Zaria as the raw biomass fuel was cut into pieces with 3 ± 0.5 mm in diameter and 10 ± 0.5 mm in length to equalise their sizes and was feed in at 10 minutes' interval through the hopper.

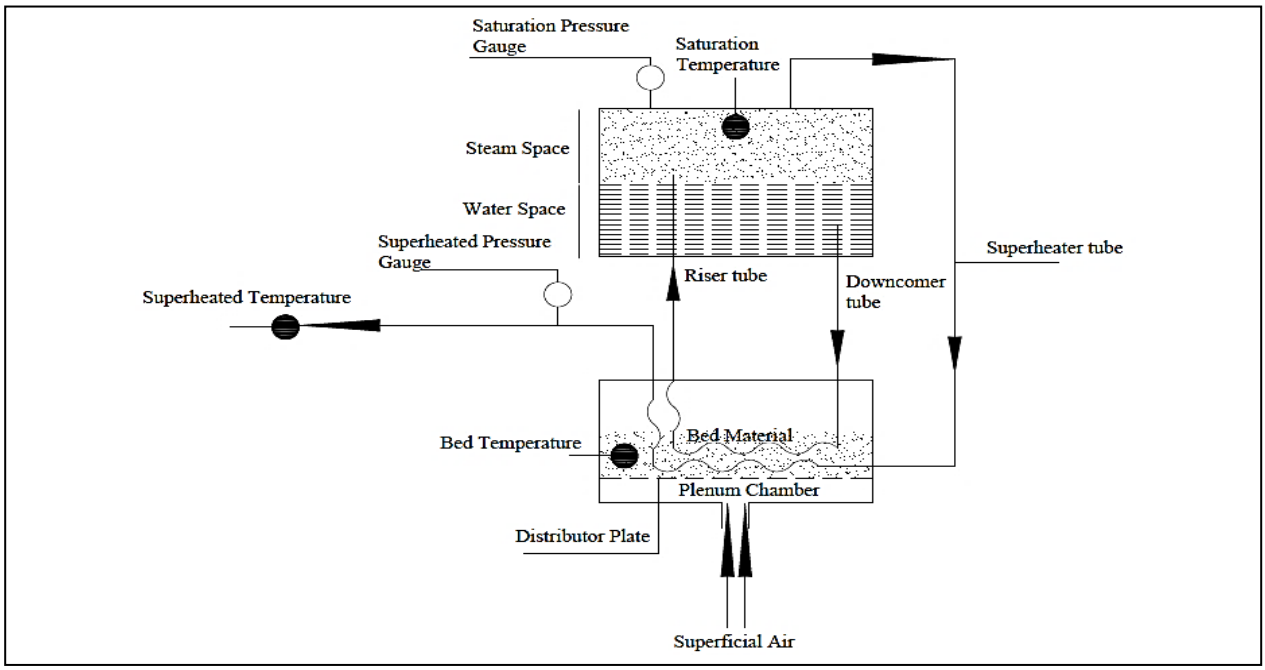


**Figure 4.** Schematic Flow Diagram of the Developed Boiler

Figure 4 shows three temperature-measuring devices that were used to determine temperatures at various points; mercury in glass thermometer ranging from 0 $^{o}$C-360 $^{o}$C was used to determine the ambient temperature as well as the initial temperature of the water. Two digital thermometers (Kane-May and MASTERTECH multipurpose clamp meter) with thermocouple wire props having one connected to the outlet of the super-heater tube, one buried in the bed to determine the bed temperature, one inserted in the steam drum to determine the saturated temperature and the last one connected to the exhaust pipe to determine the temperature of the flue gases at every 5-minutes interval.

## 3. Results and Discussion

The combustion of agricultural residue (corncobs) in the developed fluidised bed boiler are described in this section. The influences of operating parameters such as; the effect of pressure, effect of temperature as a function of time, steam generated with respect to bed heights, and emission characteristics are discussed.

### 3.1 Saturation Temperature of Steam

The temperatures of the steam at the steam drum with respect to time were taken at 5 minutes' interval. According to literature, a denser material and larger volume of bed height required more bed pressure to equalise the gravity force for fluidisation (Hilal et al., 2001). It was deduced from Figure 5 that the saturation temperature of water in the steam drum increases with increase in time; subsequently, from the bed heights of 77 mm, 47 mm and 27 mm. There was a noticeable change at 10 minutes in the temperature. This can be said to be attributed to heat gain by the water.

In addition, there was a rapid change in temperature at 25 minutes this is attributed to phase change of water from liquid to vapour. Temperature stability was attained in the bed height of 27 mm at 30 minutes from temperature ramp of 153 $^{o}$C to 155 $^{o}$C compare to bed height of 47 mm and 77 mm which were at 40 minutes and 45 minutes which were in temperature ramp of 142 $^{o}$C to 144 $^{o}$C and 117 $^{o}$C to 121 $^{o}$C, respectively. This behavior is attributed to complete bubble fluidisation of the crystalline material and the specification of the blower being able to provide enough buoyant force of fluidization (see Figure 5).

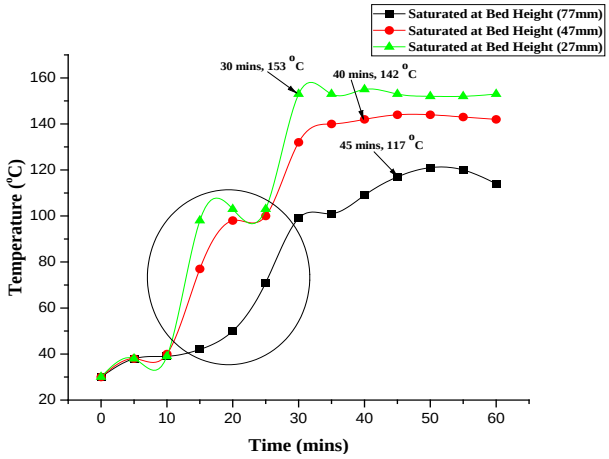


**Figure 5** Saturation Temperature of Steam/Bed Height as a Function of Time

### 3.2 Saturation Pressure of Steam

Pressure developed is a major parameter in any designed boiler (Zhong et al., 2006), Figure 6 presents the saturated pressure obtained which revolve round the designed pressure. Saturation pressures of the steam from steam drum at 5 minutes' interval were taken. It shows that the maximum saturation pressure obtained from the three experiments carried out was 3.7 bar.

The pressures obtained are 2.0 bar from 50 to 55 minutes for bed height of 77 mm, 2.1 bar from 45 to 50 minutes for bed height of 47 mm and lastly, 3.6 to 3.7 bar was obtained from 45 to 55 minutes for bed height 27 mm.

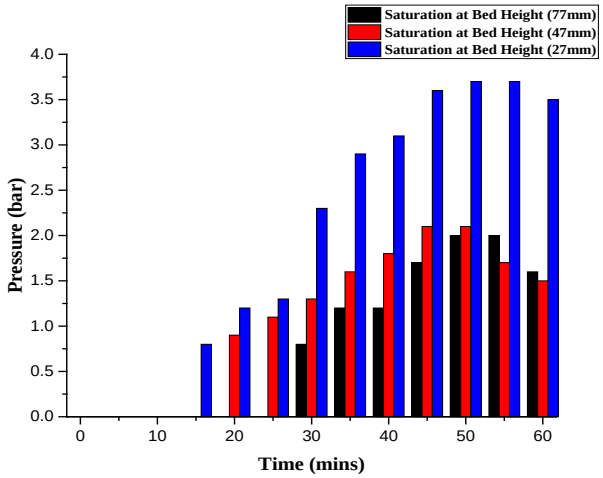


**Figure 6.** Saturation Pressure of Steam/Bed Height as a Function of Time

### 3.3 Amount of Steam Generated

Figure 7 shows the plot of the amount of steam generated in kg/h in the steam drum of the developed fluidised bed boiler. The figure revealed that 5.6 kg/h of steam was achieved from bed height of 77 mm, 6 kg/h was achieved from 47 mm and 6.6 kg/h as maximum capacity of steam achievable from the bed height of 27 mm and this is capable to run a small steam turbine, sterilisation of medical equipment, laundry and soil steaming for pest control.

### 3.4 Flue Gas Temperature at Exhaust Pipe

Figure 8 shows the flue gas temperature of the developed fluidised bed. The initially measured temperature of the bed at the onset of fluidisation was 51 $^{o}$C for bed height of 77 mm, 86 $^{o}$C for bed height of 47 mm and 89 $^{o}$C for bed height of 27 mm respectively. Conversely, it increases with increase in time (Folayan et al., 2015) up to 45 minutes, at 50 minutes a drop in temperature begins to set in and this is because of fuel stoppage.

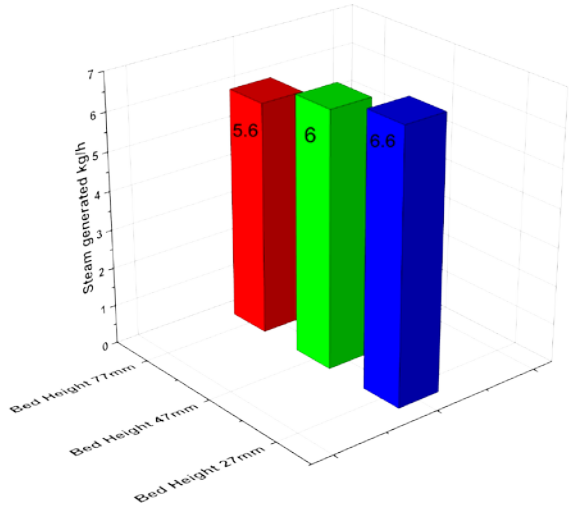


**Figure 7.** Steam Generated as a Function of Bed Height

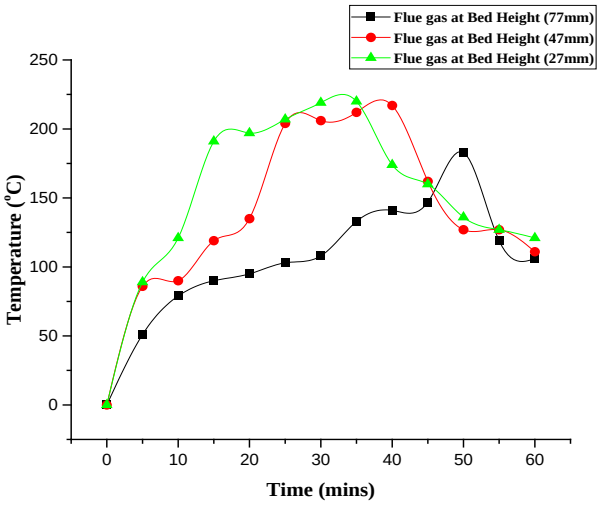


**Figure 8.** Flue Gas Temperature as a Function of Time

### 3.5 Analysis of Flue Gas Emission

The exhaust flue gas of the developed boiler is presented below after being analysed with a flue gas analyser. Figure 9 presents the exhaust emission in their percentages to be 0.001% of hydrocarbon, 0.0003% for oxides of nitrogen, 0.02% of carbon monoxide, 0.04% of carbon dioxide.

The harmful emissions were very low and this is attributed to granular material which is crystalline in nature that absorbs the harmful gas within it (Thenmozhi and Sivakumar, 2013). The excess nitrogen that was present for the combustion was found to be 0.93%. In conclusion, the oxides of Sulphur were found to be zero and this can be said to be attributed to low contents of Sulphur in biomass fuel.

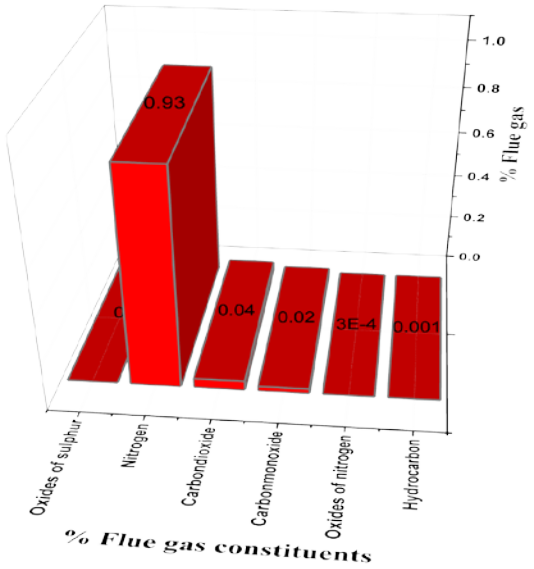


**Figure 9.** Percentage Composition of the Flue Gas Constituent

## 4. Conclusions

Fluidised bed technologies are proving to be the most practical option for biomass conversion. The fabrication of the boiler was successfully accomplished based on the design specifications of length of steam drum to be 1 m, diameter of 0.6 m, the length of the steam tubes of 3 m and diameter of 0.0127 m, respectively. Local mild steel and galvanised steel were sourced for the fabrication owing to the fact they have heat resistance and corrosion resistance.

The result of the performance evaluation showed that the bed height of 27 mm gives a better fluidisation result. Stability in the saturation temperature of steam was observed at 30 minutes up to 60 minutes with corresponding temperature ramp of 153 $^{o}$C to 155 $^{o}$C. The efficiency of the boiler was found to be 53.69% for bed height of 77 mm, 57.42% for bed height of 47mm and 61.72% for bed height of 27 mm. This shows that the developed fluidised bed boiler has its application in medium capacity steam turbine.

## References:

Armesto, L., Bahillo, A., Veijonen, K., Cabanillas, A., and Otero, J. (2002), "Combustion behaviour of rice husk in a bubbling fluidised bed", *Biomass and Bioenergy*, Vol.23, No.3, pp.171-179.

Balogun, M. B., Kulla, D. M., and Anafi, F. O. (2016), "Design and construction of an agricultural solid waste fluidised bed boiler for steam generation", *Proceedings of the 29th International Conference and Annual General Meeting of Nigerian Institution of Mechanical Engineers*, Uyo, Akwa Ibom, Nigeria, 18-21 October, pp.1-19

Boiler, A., and Code, P. V. (1989), *Rules for Construction of Pressure Vessels*, American Society of Mechanical Engineers, 1992 (1995), pp.1998-2001.

Christensen, B. (2011), *Design and Performance of a Bench-Scale Steam Fluidised Gasifier for Biomass Analysis*, M.Sc dissertation, The University of Utah.

Folayan, C. O., Pam, G. Y., and Habib, Y. B. (2015), "Fluidised combustor: Toward alternative way of energy recovery in rural Nigeria", *Journal of Energy Technologies and Policy*, Vol.5, No.2, pp.14-27.

Ganapathy, V. (2003), I*ndustrial Boilers and Heat Recovery Steam Generators: Design, Applications and Calculations*, 10th edition, Marcel Dekker, New York

Hilal, N., Ghannam, M. T., and Anabtawi, M. Z. (2001), "Effect of bed diameter, distributor and inserts on minimum fluidisation velocity", *Chemical Engineering and Technology*, Vol.24, No.2, pp.161-165.

Khan, A., De Jong, W., Jansens, P., and Spliethoff, H. (2009), "Biomass combustion in fluidised bed boilers: potential problems and remedies", *Fuel Processing Technology*, Vol.90, No.1, pp.21-50.

Khurmi, R. S., and Gupta, J. K. (2005), *A Test Book of Machine Design*, 15th edition, Eurasia Publishing House (PVT) Limited, Ram Nagar, New Delhi.

Kyauta, E., Adisa, A., Abdulkadir, L., and Balogun, S. (2015), "Production and comparative study of pellets from maize cobs and groundnut shell as fuels for domestic use", *Carbon*, Vol.14, pp.97-102.

Martínez, I., Murillo, R., Grasa, G., Rodríguez, N., and Abanades, J. (2011), "Conceptual design of a three fluidised beds combustion system capturing $CO_2$ with CaO", *International Journal of Greenhouse Gas Control*, Vol.5, No.3, pp.498-504.

Nag, P. K. (2008), *Power Plant Engineering*, 3rd edition, Tata McGraw-Hill Publishing Company Limited, New Delhi

Odigure, J., Abdulkareem, A., and Asuquo, E. (2005), "Effect of water quality on the performance of boiler in Nigerian petroleum industry", *Leonardo Electronic Journal of Practices and Technologies*, Vol.4, No.7, pp.41-48.

Ohijeagbon, I., Waheed, M., Jekayinfa, S., and Opadokun, O. (2013), "Developmental design of a laboratory fire-tube steam boiler", *Acta Technica Corviniensis - Bulletin of Engineering*, Vol.6, No.1, pp.147.

Rajput, R. K. (2010), *Thermal Engineering*, 5th edition, S. Chand and Company Limited, New Delhi.

Saidur, R., Abdelaziz, E., Demirbas, A., Hossain, M., and Mekhilef, S. (2011), "A review on biomass as a fuel for boilers", *Renewable and Sustainable Energy Reviews*, Vol.15, No.5, pp.2262-2289.

Thenmozhi, G., and Sivakumar, L. (2013), "A survey on circulating fluidised combustion boiler", *International Journal of Advanced Research in Electrical, Electronics and Instrumentation Engineering*, Vol.2, No.8, pp.4032-4042.

Varol, M., Atimtay, A. T., and Olgun, H. (2014), "Emission characteristics of co-combustion of a low calorie and high-sulfur-lignite coal and woodchips in a circulating fluidised bed combustor: Part 2. Effect of secondary air and its location", *Fuel*, Vol.130, pp.1-9.

Zhong, W., Chen, X., and Zhang, M. (2006), "Hydrodynamic characteristics of spout-fluid bed: Pressure drop and minimum spouting/spout-fluidising velocity", *Chemical Engineering Journal*, Vol.118, No.1, pp.37-46.

Zhou, D., Dong, S., Wang, H., and Bi, H. T. (2008), "Minimum fluidisation velocity of a three-phase conical fluidised bed in comparison to a cylindrical fluidised bed", *Industrial and Engineering Chemistry Research*, Vol.48, No.1, pp.27-36.

## Authors' Biographical Notes:

Muyideen B. Balogun *is Lecturer at the Department of Mechanical Engineering, Ahmadu Bello University, Zaria, Nigeria. He graduated with a B.Eng and M.Sc in Mechanical Engineering at the Ahmadu Bello University, Zaria, specialising in energy studies. His research interests include Thermal Engineering, Energy Systems, and Internal Combustion Engines. Engr. Balogun*

*is a member of the Nigerian Society of Engineers (NSE), Nigerian Institution of Mechanical Engineers (NIMechE) and a registered engineer with the Council for the Regulation of Engineering Practices in Nigeria (COREN).*

Clement O. Folayan *is Professor of Mechanical Engineering at Ahmadu Bello University, Zaria, Nigeria. He graduated with B.Eng Mechanical Engineering at Ahmadu Bello University in 1969 and then proceeded to Imperial College where he was bagged with M.Sc and Ph.D in Mechanical in 1976, specialising in energy studies. Prof. Folayan held the position of Head of Department of Mechanical Engineering and the Dean of the Faculty of Engineering at Ahmadu Bello University, Zaria from 1987 to 1992. He is a member of the Nigerian Society of Engineers (NSE), Materials Society of Nigeria (MSN), and is a registered engineer with the Council for the Regulation of Engineering Practices in Nigeria (COREN).*

Dangana M. Kulla *is Associate Professor at Ahmadu Bello University, Zaria, Nigeria. He had his first degree education at the Ahmadu Bello University, Zaria where he bagged B.Eng., and then proceeded to Bayero Universityy for his M.Sc., and Ph.D degrees in Mechanical Engineering, specialising in Energy Studies. Dr Kulla is the Managing Editor of African Journal of Renewable and Alternative Energy. His research interests include, Renewable Energy and Energy Systems. He is a member of the Nigerian Society of Engineers (NSE), and is a registered engineer with the Council for the Regulation of Engineering Practices in Nigeria (COREN).*

Fatai O. Anafi *is Associate Professor and currently Head of Department at the Department of Mechanical Engineering, Ahmadu Bello University, Zaria, Nigeria. He had his university education at the Ahmadu Bello University, Zaria where he bagged B.Eng., M.Sc., and Ph.D degrees in Mechanical Engineering, specialising in Energy Studies. His research interests include Energy Systems, Renewable Energy and Engineering Management. Dr. Anafi is a member of the Nigerian Society of Engineers (NSE), Materials Society of Nigeria (MSN), and is a registered engineer with the Council for the Regulation of Engineering Practices in Nigeria (COREN).*

Samaila Umaru *is a Senior Lecturer at Ahmadu Bello University, Zaria, Nigeria. He is the first Ph.D graduate in Automotive Engineering at Central South University, Changsha China in 2014. He has been working at Ahmadu Bello University, Zaria, since 2014. Dr. Umaru worked at Federal University of Technology (now Modibbo Adama University of Technology) Yola before joining ABU, Zaria. His research interests include Energy Engineering, Virtual Reality and Materials Development. He is a member of the Nigerian Society of Engineers (NSE), International Society of Offshore and Polar Engineers (ISOPE), and is a registered engineer with the Council for the Regulation of Engineering Practices in Nigeria (COREN).*

Nua O. Omisanya *is Lecturer at Ahmadu Bello University, Zaria, Nigeria. He had his first degree in Mechanical Engineering at University of Ibadan. He joined the defunct Centre for Automotive Design and Development (CADD) in 1992, which is now National Automotive Design and Development (NADDC). He bagged his M.Sc., at Bayero Universityy and Ph.D degrees in Mechanical Engineering at Ahmadu Bello University, Zaria, specialising in Energy Studies. Dr. Omisanya is a recipient of 2010 Innovator of Tomorrow Grant Award. He is a member of the Nigerian Society of Engineers (NSE), Nigerian Institution of Mechanical Engineers (NIMechE) and a registered engineer with the Council for the Regulation of Engineering Practices in Nigeria (COREN).*

■